ANTIOXIDANTS & REDOX SIGNALING
Volume 5, Number 5, 2003

Original Research Communication

Formation of Disulfide Bond in p53 Correlates with Inhibition of DNA Binding and Tetramerization

XIU ZHU SUN,[1] CHRISTOPHER VINCI,[1] LINNA MAKMURA,[1] SHUBO HAN,[1] DUNG TRAN,[1] JOHN NGUYEN,[1] MICHAEL HAMANN,[2] SANDRA GRAZZIANI,[1] SHELETHER SHEPPARD,[1] MARGARITA GUTOVA,[1] FEIMENG ZHOU,[1] JAMES THOMAS,[2] and JAMIL MOMAND[1]

ABSTRACT

The p53 tumor suppressor protein is susceptible to oxidation, which prevents it from binding to its DNA response element. The goal of the current research was to determine the nature of the cysteine residue thiol oxidation that prevents p53 from binding its DNA target and its effect on p53 structure. Recombinant p53, purified in the presence of the reducing agent dithiothreitol (DTT), contains five free thiol groups on the surface of the protein. In the absence of DTT, p53 contains only four thiol groups, indicating that an average of one surface thiol group is readily susceptible to oxidation. Sulfite-mediated disulfide bond cleavage followed by reaction with 2-nitro-5-thiosulfobenzoate showed that oxidized p53 contains a single disulfide bond per monomer. By atomic force microscopy, we determined that reduced p53 binds to a double-stranded DNA containing the p53 promoter element of the *MDM2* gene. The DNA-bound reduced p53 has an average cross-sectional diameter of 8.61 nm and a height of 4.12 nm. The amount of oxidized p53 that bound to the promoter element was ninefold lower, and it has an 18% larger average cross-sectional diameter. Electromobility shift assays showed that binding of oxidized p53 to DNA was enhanced upon addition of DTT, indicating that oxidation is reversible. The possibility that oxidized p53 contained significant amounts of sulfenic (−SOH), sulfinic ($-SO_2H$), or sulfonic acid ($-SO_3H$) was ruled out. Gel filtration chromatography indicated that oxidation increases the percentage of p53 monomers and high-molecular-weight oligomers (>1,000 kDa) relative to tetrameric p53. Protein modeling studies suggest that a mixed disulfide glutathione adduct on Cys182 could account for the observed stoichiometry of oxidized thiols and structural changes. The glutathione adduct may prevent proper helix–helix interaction within the DNA binding domain and contribute to tetramer dissociation. *Antioxid. Redox Signal.* 5, 655–665.

INTRODUCTION

THE P53 TUMOR SUPPRESSOR is a checkpoint protein that elicits cell-cycle arrest, DNA repair, and apoptosis in response to stressors. Its importance is underscored by the fact that its gene is mutated in ~30–50% of human cancers (22). Cells lacking sufficient levels of p53 are prone to uncontrolled proliferation resulting from activating mutations in protooncogenes and inactivating mutations in tumor suppressor genes (16). On the other hand, mice engineered to express high levels of active p53 exhibit a shortened life span accompanied by aging-associated phenotypes, such as osteoporosis and organ atrophy (28). Cells expressing elevated levels of p53 may be subject to premature apoptosis and, therefore, may not be available to replenish differentiated cells within organs that undergo atrophy late in life. Thus, a delicate balance between high and low levels of p53 is necessary for cancer-free survival to old age. To perform its tumor suppressor

[1]Department of Chemistry and Biochemistry, California State University, Los Angeles, CA.
[2]Department of Biochemistry, Iowa State University, Ames, IA.

activity, p53 binds, as a tetramer, to DNA elements within promoters of its target genes and enhances transcription (9, 30). In cancers, mutations that arise within the *p53* gene usually code for amino acid replacements that curtail the ability of p53 to bind DNA (17). These mutations can disrupt p53/DNA complex formation by creating amino acid substitutions at sites that contact the DNA element or by creating substitutions at sites required for tertiary structure maintenance (4).

Aside from mutations, the DNA binding property of p53 can be prevented by oxidation (6, 11), evidenced by the fact that binding of p53 to DNA *in vitro* can be enhanced by the addition of the reducing agent dithiothreitol (DTT) (13). As DTT can reduce cysteine residue disulfide bonds and p53 is predicted to have several cysteine thiol groups on the protein surface, it has been proposed that these thiol groups could be susceptible to redox regulation (31). Cysteine thiol groups appear to be critical for binding to DNA because thiol blocking agents (11, 23) and certain cysteine residue amino acid replacements (2, 3) inhibit binding of p53 to DNA. p53 consists of three major domains. The N-terminal 100 amino acids comprise the transactivation domain; the central 200 amino acids comprise the DNA binding domain; and the remaining amino acids at the C-terminus comprise the tetramerization domain and other regulatory functions. All 10 cysteine residues of human p53 lie within the DNA binding domain.

p53 is also susceptible to redox regulation within cells. Recent work has shown that p53 is susceptible to oxidation by copper loading in cultured cells (10, 31). Copper leads to increased susceptibility to Fenton chemistry-induced hydroxyl radical production, which appears to oxidize p53 cysteine thiol groups. UV light and ionizing radiation may also lead to p53 oxidation because such treatments prevent p53 within nuclear lysates from binding DNA unless it is first treated with a reducing agent (2). Thioredoxin, a small protein that transfers electrons to disulfide bonds, increases p53-mediated transactivation (29). These data indicate that, under certain circumstances, p53 is susceptible to thiol group oxidation and that oxidation results in alteration of its DNA binding properties within cells. A major hindrance to the study of p53 redox regulation is the lack of knowledge as to the type of cysteine thiol group oxidation that occurs. Disulfide bond, sulfenic acid, sulfinic acid, and sulfonic acid formation are among the possibilities, although the latter two are unlikely candidates because they are not capable of reduction by DTT. In this report, we present evidence that p53 has the propensity to form a disulfide bond under mild oxidizing conditions. The presence of a disulfide bond correlates with disruption of the tetrameric nature of p53 and inhibition of DNA binding.

EXPERIMENTAL PROCEDURES

Materials

All chemicals were purchased from Sigma–Aldrich (St. Louis, MO, U.S.A.) or Fisher Scientific (Tustin, CA, U.S.A.) unless otherwise noted. Sodium borohydride was obtained from Matheson Coleman & Bell Manufacturing Chemists (Norwood, OH, U.S.A.). Si(100) wafers were acquired from Silicon Valley Microelectronics Inc. (San Jose, CA, U.S.A.). All custom oligonucleotides were purchased from Integrated DNA Technologies (Coralville, IA, U.S.A.). For atomic force microscopy (AFM) studies, a 25mer oligonucleotide with its 5' end modified with an aminoheptyl tether group [5'-AGT TAA GTC CTG ACT TGT CTC CCC C $(CH_2)_7NH_2$-3'] and its 20mer complementary strand (5'-AGA CAA GTC AGG ACT TAA CT-3') were used. For electromobility shift assays, a 30mer oligonucleotide (5'-AAT TCT CGA GCA GAA CAT GTC TAA GCA TGC TGG GCT CGA G-3') and its 30mer complementary strand were used.

Purification of recombinant human p53

Recombinant p53 was purified from Sf9 insect cells infected with baculovirus expressing full-length human p53, as previously described (18). Buffer A (40 m*M* Tris-HCl, pH 8.0, 0.4 *M* NaCl, 1 m*M* DTPA) was used to elute p53−DTT from the Q-Sepharose Fast Flow anion-exchange column. Buffer A plus 10 m*M* DTT was used to elute p53+DTT from the anion-exchange column. Protein purity was assessed by Coomassie staining of sodium dodecyl sulfate–polyacrylamide gel electrophoresis (SDS-PAGE) gels, and protein quantity was assessed by comparison of protein band density to known quantities of bovine serum albumin unless otherwise noted.

Procedures for the substrate surface treatment, DNA immobilization, and p53 attachment

Si(100) substrates, cut from a large wafer to 1.0 cm × 1.0 cm squares, were sonicated in chloroform and rinsed with deionized water. The wafers were then dipped in an aqueous solution containing 14% (wt/vol) NH_4OH and 14% (vol/vol) hydrogen peroxide at 68°C for 15 min. Upon rinsing with deionized water and drying, the wafers were immersed in a 5% (wt/vol) aminopropyltriethoxysilane (APTES) aqueous solution for 30 min for surface modification. The excess APTES was removed by successive washes of toluene, a 50:50 mixture of toluene and ethanol, and absolute ethanol. These APTES-covered wafers were dried *in vacuo* at room temperature as previously described (21). To immobilize the oligonucleotides onto the APTES molecules, 50 µl of 0.1 *M* Na_2HPO_4, pH 7.0, 2.5% (wt/vol) glutaraldehyde was cast onto the wafer surfaces and allowed to incubate for 15 min. Following an extensive washing step as described previously (19), the wafers were soaked in 10 m*M* Tris-HCl, pH 7.4, 1 m*M* EDTA, 0.1 *M* NaCl (TE-NaCl buffer), which contained 1 µ*M* 25mer oligonucleotide. After drying for 12 h at room temperature (~25°C) and <30% relative humidity, the wafers were vigorously rinsed with a 0.2% (wt/vol) SDS aqueous solution to remove the unbound oligonucleotide. The unreacted amino groups on the wafer surface were deactivated with freshly prepared 68 m*M* $NaBH_4$ prepared in 30% (vol/vol) ethanol. The wafer surfaces were again thoroughly rinsed with 0.2% SDS. Hybridization with the complementary 20mer was accomplished by immersing the substrate surface in TE-NaCl buffer containing 1 µ*M* target DNA for 12 h at room temperature. The attachment of the p53 molecules was achieved by exposing the dsDNA

molecules on the surfaces to 8 μg/ml p53 in buffer A for 15 min at 4°C. The surfaces were rinsed successively 1 min each with water, 0.2% (wt/vol) SDS, and water.

AFM instrument

AFM images were collected using an AFM equipped with a magnetic alternating current mode (MAC-mode AFM; Molecular Imaging, Phoenix, AZ, U.S.A.). The MAC cantilever tips (Molecular Imaging) had a spring constant of 2.8 N/m and a resonance frequency of ~75 kHz. Images were scanned across a 600 cm × 600 nm^2 surface area for 120 reduced p53/DNA complexes and 23 oxidized p53/DNA complexes. Particle diameter and height were measured using the Picoscan software program (version 4.18; Lot-Oriel, U.K.).

Disulfide bond quantification

Quantification of disulfide bonds was performed as described (26). In brief, equal volumes of 7.5 μ*M* p53−DTT in 40 m*M* Tris-HCl, pH 7.6, 400 m*M* NaCl, and alkylating/denaturing reagent were mixed and allowed to incubate 1 h at room temperature. The alkylating/denaturing agent was 80 m*M* *N*-ethylmaleimide, 6 *M* guanidine isothiocyanate (Gu-SCN) dissolved in buffer B (40 m*M* Tris-HCl, pH 9.5, 400 m*M* NaCl). This p53 solution was then dialyzed against buffer B 166,000-fold. Solid Gu-SCN was added to p53 to a final concentration of 3 *M,* and the p53 was concentrated on a Centricon-30 ultrafiltration unit until its final concentration was 15 μ*M*. A 400-μl aliquot of 2-nitro-5-thiolsulfobenzoate (NTSB) assay solution (0.5 m*M* NTSB, 0.2 *M* Tris, 0.1 *M* Na_2SO_3, 3 m*M* EDTA, and 3 *M* Gu-SCN) was added to 115 μl of 15 μ*M* p53, and absorbance at 412 nm was measured at 2-min intervals. Within 14 min, the absorbance maximum was observed and held steady until 26 min after which the experiment was terminated. Flow-through solution from the ultrafiltration unit was used as background for absorbance measurements. Oxidized glutathione and bovine RNase A were the positive controls for disulfide bond quantification. The concentration of p53 was calculated from the theoretical extinction coefficient of 38,347 M^{-1} cm^{-1} at 280 nm. The concentration of 2-nitro-5-thiobenzoic acid (NTB) produced in the reaction was calculated from its extinction coefficient of 13,600 M^{-1} cm^{-1} at 412 nm.

Protein thiol group quantification

p53−DTT and p53+DTT were separately dialyzed in 0.01 *M* KH_2PO_4, pH 7.6, 1 m*M* EDTA (dialysis buffer). The p53+DTT solution was dialyzed to the point that the final DTTconcentration was 20 μ*M* to prevent oxidation of p53 during dialysis. The p53+DTT solution was concentrated to 20 μ*M* p53 monomer with a Centricon 30 ultrafiltrator and then diluted to 7.5 μ*M* with dialysis buffer. The p53−DTT was prepared identically. A 13-μl aliquot of 5,5'-dithiobis(2-nitrobenzoicacid) (DTNB) solution (10 m*M* DTNB, 0.1 *M* NaH_2PO_4, pH 8.0) was added to 400 μl of p53, and absorbance measurement of NTB at 412 nm was recorded after 15 min. The final p53 concentration was always ~5 μ*M*. The background absorbance was obtained from the flow-through of the ultrafiltrator diluted in the same manner as the concentrated p53. Positive controls for thiol group quantification were bovine serum albumin and 2-mercaptoethanol.

Sulfenic acid analysis

Sulfenic acid analysis was performed as previously described (14). This assay relies on the fact that 4-chloro-7-nitrobenz-2-oxa-1,3-diazole (NBD chloride) forms an NBD adduct with sulfenic acid to give an absorbance maximum at 347 nm (extinction coefficient of 13,400 M^{-1} cm^{-1}) (7). If NBD forms an adduct with a thiol, an absorbance maximum at 420 nm (extinction coefficient of 13,000 M^{-1} cm^{-1}) is observed. In brief, the p53−DTT solution buffer was exchanged with buffer C (50 m*M* K_2HPO_4, pH 7.0, 1 m*M* EDTA) by ultrafiltration with Centricon plus-20 (Millipore). The p53−DTT solution at a final concentration of 18 μ*M* was reacted with 200 μ*M* NBD for 30 min at room temperature. To remove unreacted NBD, p53 was repeatedly diluted 30-fold with buffer C and reconcentrated to 500 μl three times. Using the last flow-through as background, the UV-VIS spectrum was measured. Significant NBD adduct absorbance was detected at 420 nm, but not at 347 nm, indicating that the p53−DTT free thiol groups reacted with NBD, but no sulfenic acid was present. The final p53 concentration observed was 18 μ*M,* as quantified by absorption at 280 nm.

Sulfinic and sulfonic acid analysis

p53 samples were analyzed for sulfinic and sulfonic acid as described (12). In brief, samples were incubated at 37°C for 15 min in buffer containing 120 m*M* sodium phosphate buffer, pH 7.4, 7 *M* urea, and 10 m*M* DTT. Cysteine residues were then blocked with 40 m*M* iodoacetamide. Each sample was split into two fractions, one of which was treated with 10 m*M* HOCl for 5 min at room temperature in order to oxidize sulfinic acids to sulfonic acids. The reactions were terminated after 5 min with the addition of 30 m*M* DTT. The samples were extensively dialyzed and hydrolyzed by vapor phase acid. Amino acid analysis was conducted using precolumn derivatization with *o*-phthalaldehyde and reverse-phase HPLC. HOCl converts sulfinic to sulfonic acid; therefore, the amount of cysteic acid found in a sample treated with HOCl represents the total protein irreversibly oxidized cysteine. Cysteic acid found in samples not treated with HOCl represents the amount of cysteine detected as protein sulfonic acid. Protein sulfinic acid was calculated by subtracting the total protein sulfonic acid from the total irreversibly oxidized cysteine. The total moles of p53 in a hydrolysate was calculated on the basis of total leucine in the p53 sample (32 mol of leucine/mol of p53).

p53 thiol group accessibility analysis by methoxymaleimide polyethylene glycol (MAL-PEG) reactivity

p53+DTT was dialyzed against 40 m*M* Tris-Cl, pH 8.0, 400 m*M* NaCl, 0.1 m*M* DTT for 16 h at 4°C to lower the DTT concentration so that it would not block MAL-PEG modification reaction. p53 at a final concentration of 2 μ*M* was incu-

bated with 0.67 m*M*, 1.3 m*M*, or 3 m*M* MAL-PEG in 27 m*M* Tris-Cl, pH 8.0, 270 m*M* NaCl for 30 min at 25°C (p53−DTT contained 67 μ*M* DTT in the final reaction). Reactions were quenched by the addition of Laemmli sample buffer [0.125 *M* Tris-Cl, pH 6.8, 1 *M* 2-mercaptoethanol, 20% (vol/vol) glycerol, 0.02% (wt/vol) bromphenol blue, 10% (vol/vol) 2-mercaptoethanol, 20% (wt/vol) SDS] heated to 100°C. Samples were separated on an 8% cross-linked SDS-polyacrylamide gel and subjected to western blotting with DO-1 antibody (Oncogene Science, San Diego, CA, U.S.A.) as previously described (18). Densitometry of scanned gel images was performed with UN-SCAN-IT gel software (version 5.1, Silk Scientific Corp., Orem, UT, U.S.A.).

Gel filtration

p53+DTT (94 μl, 0.5 mg/ml) or p53−DTT (94 μl, 0.33 mg/ml) was injected onto a 300 × 7.8 mm Bio-Sil SEC 400-5 HPLC column, 5 μm particle size (Bio-Rad) equilibrated with 100 m*M* NaH_2PO_4, pH 7.06, 1 m*M* EDTA. The HPLC consisted of a Varian 9050 UV/VIS detector, a Varian 9012 pump, and a Varian 9100 autosampler. The flow rate was 1 ml/min, and the p53 elution profile was monitored at a wavelength of 280 nm. Relative levels of protein were determined by integration of areas under the peaks. The protein molecular weight (MW) standards from Bio-Rad (catalog no. 151-1901) consisted of bovine thyroglobulin (670,000), bovine γ-globulin (158,000), chicken ovalbumin (44,000), horse myoglobin (17,000), and vitamin B-12 (1,350). The correlation coefficient of the relationship between the MW and elution periods of the protein standards was 0.946.

Electromobility gel shift analysis

Complementary single-stranded oligonucleotides containing the p53 binding portion of the *GADD45* promoter sequence were annealed in TE (10 m*M* Tris-HCl, pH 8.0, 1 m*M* EDTA) at a final concentration of 1 μg/μl. The oligonucleotide probe at 0.02 μg/μl was end-labeled in the presence of 0.45 mCi of [γ-^{32}P]ATP (6,000 Ci/mmol) (Perkin-Elmer) with 20 units of T4 polynucleotide kinase (New England BioLabs) in 70 m*M* Tris-HCl, pH 7.6, 10 m*M* $MgCl_2$, 5 m*M* DTT for 10 min at 37°C. The reaction was quenched by the addition of EDTA from a 0.5 *M,* pH 8.0, stock solution, to a final concentration of 0.01 *M*. Radiolabeled probe was separated from unreacted ATP by G-50 spin column (Roche Molecular Biochemicals; catalog no. 1 273 965) centrifuged at 1,100 × *g* for 4 min at room temperature. A 1-μl aliquot of eluant was used to measure efficiency of labeling by liquid scintillation counting. The probe was diluted with TE to a final concentration of 6,000 cpm/μl prior to each experiment.

For electromobility shift assay, p53 at a final concentration of 44–111 ng/μl was preincubated for 10 min at room temperature with 74 ng/μl poly(dI-dC)•poly(dI-dC) in 10 m*M* Tris-HCl, pH 7.5, 50 m*M* NaCl, 0.5 m*M* EDTA, 1 m*M* $MgCl_2$, and 4% (vol/vol) glycerol. Where indicated, DTT was added to a final concentration of 0.5 m*M*. After preincubation, 2 μl of 6,000 cpm/μl radiolabeled probe was added and the mixture was allowed to incubate 20 min at room temperature. The reaction was quenched by the addition of 2 μl of 250 m*M* Tris-HCl, pH 7.5, 0.2% bromphenol blue, 0.2% xylene cyanol, 40% (vol/vol) glycerol. Samples were separated on a 6% nondenaturing polyacrylamide gel at room temperature in 0.045 *M* Tris, 1 m*M* EDTA, 0.044 *M* boric acid. Gels were dried and exposed to x-ray film.

Protein modeling

The crystal structure of three p53 core regions consisting of amino acids 92–292 with a segment of DNA containing the p53 consensus sequence was obtained from the Protein Data Bank (PBD ID 1TSR). Its three-dimensional image was visualized and manipulated using WebLab® ViewerPro™ software (version 4.0, Molecular Simulations Inc., San Diego, CA, U.S.A.). Of the three protein chains in the crystal structure, chain B has the most interactions with the consensus site and is thought to accurately represent the p53–DNA interaction that occurs *in vivo*. Thus, chains A and C were deleted for this model study. The DNA sequence in the crystal structure is 5'-ATAATT**GGGCA**AGTC-TAGGAA-3' (pentamer consensus site in bold face). The DNA binding domain makes several hydrogen bonds with the consensus site, notably, Lys120 with the second G, Arg280 with the G on the opposite strand, and Cys277 with the C on the opposite strand. To construct the model, a second pentamer consensus sequence of AGACT is on the opposite strand complementary to five bases in tandem to the first sequence. A second p53 core subunit was created by duplicating chain B. The new subunit was positioned in the DNA major groove so that it interacted with the second consensus sequence in the same way that protein chain B binds with the first. Glutathione molecules were created using the molecular builder tools in the software program. To simulate oxidation via glutathiolation, these molecules were bound via disulfide bonds to the Cys182 residues of the two p53 subunits.

RESULTS

Oxidized p53 contains one oxidized thiol per monomer

Crude nuclear lysate from insect cells infected with human p53 baculovirus was loaded onto an anion-exchange column, and the recombinant p53 was eluted with a salt buffer either containing or lacking the reducing agent DTT. Figure 1 is a Coomassie-stained Laemmli gel showing that p53 lacking DTT (p53−DTT) and p53 with DTT (p53+DTT) were >90% pure. We first sought to determine if p53 purified in the absence of DTT was oxidized relative to p53 purified in the presence of DTT. DTNB reactivity was used to determine the stoichiometry of solvent-exposed thiol groups per p53 polypeptide (8). Table 1 shows that, on average, five thiol groups per polypeptide reacted with DTNB in p53+DTT. We predicted that if p53−DTT were oxidized, then one or more thiol groups on the protein surface would fail to react with DTNB. Table 1 shows that approximately four thiol groups per polypeptide reacted with DTNB in p53−DTT, indicating that an average of one thiol group per p53 polypeptide was oxidized in the p53−DTT sample relative to the p53+DTT sample.

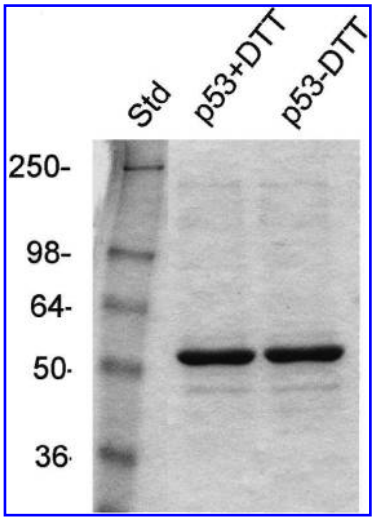

FIG. 1. Coomassie-stained gel demonstrating p53 purity in the presence and absence of DTT. Proteins eluted from Fast-Flow Q Sepharose column were separated by SDS-PAGE on an 8% cross-linked gel. MW standard sizes are shown in kilodaltons.

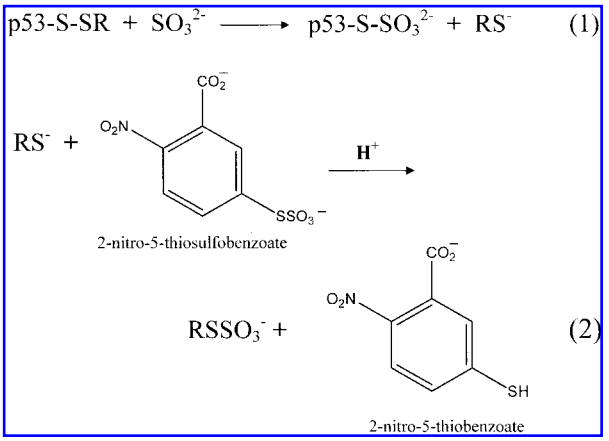

FIG. 2. Reaction mechanism for sulfite cleavage reaction of disulfide bond and quantification with NTSB.

Oxidized p53 contains one disulfide bond per monomer

We next explored the possibility that oxidized p53 contains a disulfide bond. First, oxidized p53 was treated with a denaturant and *N*-ethylmaleimide to alkylate free thiols. In this procedure, the presence of a disulfide bond is revealed if one of the two sulfur atoms in the disulfide bond reacts with sulfite to form thiosulfonate (Fig. 2, reaction 1). The remaining cleaved sulfur atom forms a free thiol (26). Subsequent reaction of NTSB with the free thiol produces a second thiosulfonate and the spectroscopically active nitrothiobenzoate (Fig. 2, reaction 2). The amount of nitrothiobenzoate produced is a direct measure of the number of disulfide bonds present in the reaction mix, and it is normalized to the number of p53 polypeptides present. Our data indicate that one disulfide linkage (1 ± 0.12, $n = 3$) is present per oxidized p53 polypeptide. To determine whether this disulfide bond connects two p53 polypeptides, the molecular size of oxidized p53 was analyzed by denaturing, nonreducing SDS-PAGE. The vast majority of the oxidized p53 migrated as a 53-kDa protein (data not shown), indicating that there was no evidence for extensive intermolecular disulfide bond formation between two or more p53 polypeptides. The demonstration of the presence of a disulfide linkage and the fact that oxidized p53 contains one less free thiol group than reduced p53 is consistent with the hypothesis that five thiol groups are located on the protein surface and that, in the absence of reducing agent, a disulfide bond is formed between an exposed thiol on the protein and a second thiol. The absence of significant levels of covalently linked subunits suggests it is likely that the second thiol is either a buried cysteine thiol in p53 or a small MW thiol ligand.

p53 is not oxidized to sulfenic acid, sulfinic acid, or sulfonic acid

We also considered the possibility that oxidized p53 may contain sulfenic acid ($-SOH$), sulfinic acid ($-SO_2H$), or sulfonic acid ($-SO_3H$). Like a disulfide bond, sulfenic acid can be reduced to the thiol by DTT (5). To determine if oxidized p53 contains sulfenic acid, it was reacted with NBD, which absorbs visible light at 347 nm when it is covalently bound to sulfenic acid (7, 14). No detectable sulfenic acid was observed in oxidized p53. However, the possibility that sulfenic acid is transiently formed during disulfide bond formation cannot be

TABLE 1. QUANTIFICATION OF SOLVENT ACCESSIBLE THIOLS ON P53

Experiment	*p53 status**	*p53 (μM)*	*SH (μM)*	*SH/p53†*
1	Reduced ($n = 5$)	5.61 ± 0.07	28.6 ± 1.59	5.09 ± 0.33
	Oxidized ($n = 5$)	4.97 ± 0.45	20.9 ± 3.60	4.19 ± 0.43
2	Reduced ($n = 3$)	5.66 ± 0.32	26.8 ± 1.16	4.75 ± 0.24
	Oxidized ($n = 3$)	5.61 ± 0.065	21.9 ± 1.35	3.90 ± 0.28

*Reduced refers to p53 purified in the presence of DTT. Oxidized refers to p53 purified in the absence of DTT. *n* is the number of independent measurements performed on a separate batch of p53 purified for each of two experiments.

†Ratio of moles of thiol groups determined by DTNB assay divided by moles of p53 monomer.

ruled out. Next, we checked whether oxidized p53 contained sulfinic acid by performing a reaction to convert sulfinic acid to cysteic acid, followed by hydrolysis and amino acid analysis (see Experimental Procedures). Oxidized p53 contains 0.1 moles (±0.02, $n = 3$) of sulfinic acid per mole of p53 polypeptide and reduced p53 contains 0.06 moles (±0.01, $n = 3$) of sulfinic acid per mole of p53 polypeptide. This indicates that the presence of DTT prevents irreversible oxidation to sulfinic acid and that the level of sulfinic acid in oxidized p53 was essentially the same as that in the reduced p53. Moreover, the absolute level of sulfinic acid in oxidized p53 is substoichiometric. The presence of sulfonic acid was also checked, but none could be detected above background levels. The data show that oxidized p53 forms an average of one disulfide per p53 polypeptide, but does not form appreciable levels of sulfenic, sulfinic, or sulfonic acid.

Addition of reducing agent enhances oxidized p53 binding to DNA

To confirm that p53 binds to DNA in a redox-sensitive manner, electromobility shift assays were performed. A synthetic radiolabeled oligonucleotide containing the *GADD45* p53-binding element was used to assess the DNA binding properties of p53. The p53/DNA complex was separated from unbound probe by gel electrophoresis, and the complex was detected by autoradiography. Figure 3A shows that oxidized p53 was unable to efficiently bind to the probe. The level of oxidized p53 that bound to the probe was only 2.2-fold over background. When DTT was added to the oxidized p53/DNA mixture, DNA binding increased to 5.4-fold (±0.3) over background. This indicates that oxidized p53 could be activated upon addition of DTT and is consistent with a model in which p53 undergoes reversible oxidation reactions on its cysteine residues. Figure 3B shows that when reduced p53 was heat-inactivated or when excess unlabeled probe was added to the reaction as a competitor, the reduced p53 failed to bind to the probe. This suggests that DNA binding requires p53 tertiary structure and that the binding is competitively inhibited. The data show that p53 requires DTT for efficient DNA binding and that oxidized p53 can be altered by DTT to bind DNA more efficiently. We also used the electromobility shift assay to test if DTT increased p53 binding to an oligonucleotide probe representing a p53 binding site within the *MDM2* promoter and observed similar results (data not shown). This indicates that p53 likely requires DTT for efficient binding to a number of p53 binding sequences in the promoters of several genes.

To extend these studies, MAC-mode AFM was used to detect p53 bound to a double strand oligonucleotide sequence representing a DNA element within the *MDM2* promoter. This method allows one to visualize the protein bound to DNA and measure its dimensions. Synthetic oligonucleotides representing the complete p53 binding site (20mer) were covalently attached to a silica surface. The DNA bound silica surface was incubated with oxidized p53 or reduced p53 for 15 min, after which the surface was washed. Figure 4A shows that when reduced p53 was added to the surface, many particles could be detected. Figure 4B shows that fewer particles were observed when an identical concentration of the oxidized form was applied to the DNA-covered surface. Importantly, no particles could be detected when p53 was not added to the bound DNA (Fig. 4C). By grain analysis, the surface density of reduced p53 particles was 5.6×10^{10} conjugates/cm^2, and the surface density of the oxidized counterpart was 6.8×10^9 conjugates/cm^2. The data show that ninefold fewer p53 conjugates were bound to the oligonucleotides in the absence of DTT. The AFM images confirm the results obtained from the electromobility shift assays and demonstrate that DTT enhances the binding of p53 to DNA. These results support a model in which oxidation reversibly inhibits the capacity of p53 to bind to DNA.

Dimensions of reduced and oxidized p53 bound to DNA

Measurement of the particle dimensions should give an estimate of the size of p53 bound to DNA. p53 is known to bind efficiently to two half-sites within the DNA as a tetramer (20, 30). Measurement of the p53 particles in the AFM images containing DTT indicates that the cross-section diameter is 8.61 nm (±1.12) and the height is 4.12 nm (±0.76) (Fig. 4D). The size of these particles is consistent with p53 acting as a tetramer with a shape that is fairly flat, in line with a recent solution NMR/modeling study (15). The low standard deviation in the size of the particles indicates that the population of DNA-bound p53 is homogeneous. Longer incubation

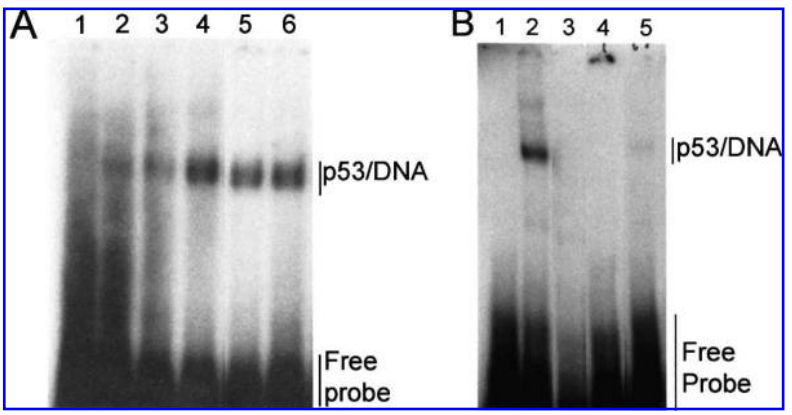

FIG. 3. Electromobility shift assays demonstrating requirement for DTT for efficient binding to *GADD45* promoter. (**A**) Electromobility shift assay demonstrating effect of DTT on DNA binding by oxidized p53. Lane 1: free probe with no added p53; lanes 2 and 3: oxidized p53; lanes 4–6: oxidized p53 plus added DTT. (**B**) Electromobility shift assay demonstrating specificity of p53 binding to DNA probe containing the sequence from the *GADD45* promoter. Lane 1: free probe (no added p53); lane 2: reduced p53; lane 3: oxidized p53; lane 4: reduced p53 (heat-inactivated); lane 5: reduced p53 with excess unlabeled competitor DNA.

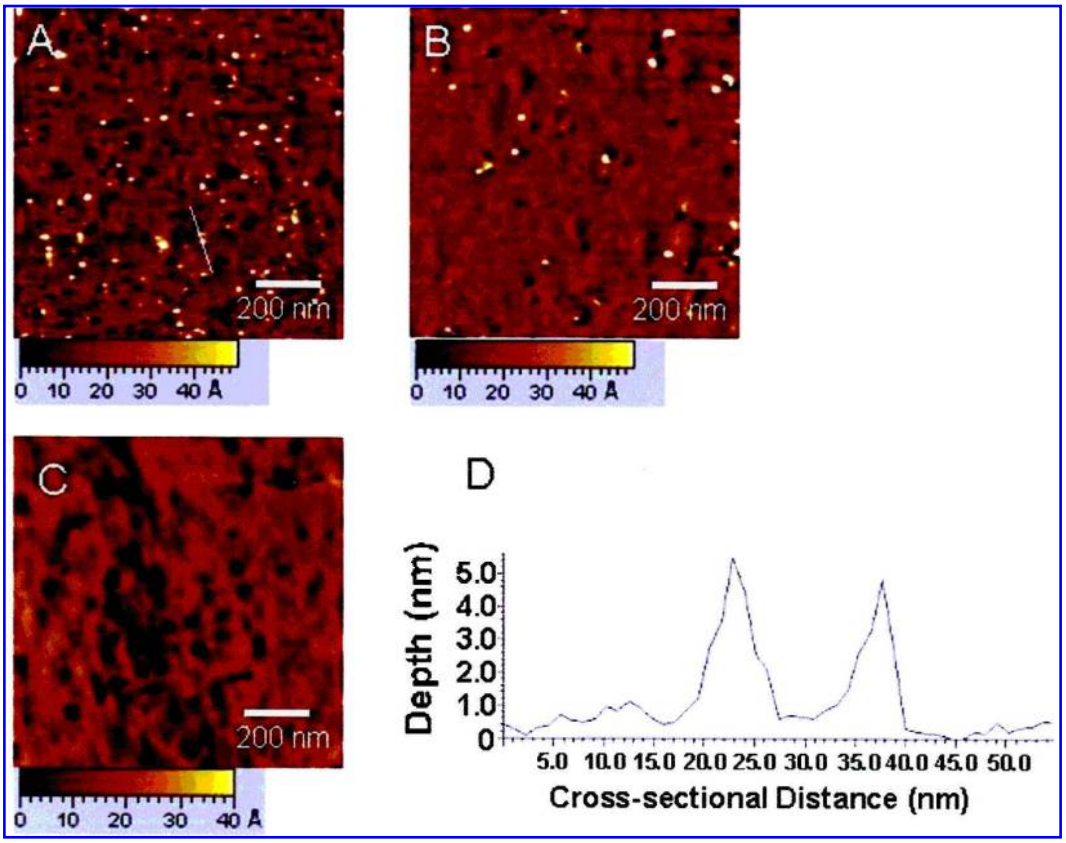

FIG. 4. MAC-mode AFM images of p53 bound to oligonucleotide probe representing *MDM2* promoter. (**A**) AFM image of reduced p53 bound to oligonucleotide probe. (**B**) AFM image of oxidized p53 bound to oligonucleotide probe. (**C**) AFM image of surface-bound oligonucleotide probe in the absence of p53. (**D**) Cross-section distance and depth dimensions of two p53 particles from image A, bisected by the white line segment.

times of p53 with the bound DNA revealed much larger particles likely due to large molecular aggregates. Oxidized p53 bound to DNA had a cross-section diameter of 15.32 nm (±2.12) and a height of 3.14 nm (±2.18). The dimensions of the oxidized p53 bound to DNA indicates that oxidized p53 may consist of higher ordered oligomers that vary in the number of bound subunits or exhibit conformations that are varied. Overall, the data indicate that the reduced p53 and oxidized p53 bound to DNA have fundamentally different sizes and that the oxidized p53 particle dimensions are more varied.

Oxidation promotes formation of monomers, dimers, and abnormal tetramers of p53

Given that oxidized p53 particle dimensions differ from reduced p53 particle dimensions, we explored the possibility that oxidation alters the oligomeric state of p53. Oxidized p53 was fractionated by gel filtration chromatography, and the elution positions of the p53 oligomers were transformed into apparent MWs by comparison with elution positions of protein standards (Table 2). This comparison assumes an overall shape that is consistent from protein to protein. The majority

TABLE 2. GEL FILTRATION CHROMATOGRAPHY ANALYSIS OF P53 + DTT AND P53−DTT

p53 + DTT		*p53 − DTT*	
Apparent MW (kDa)	Relative percentage (%)	Apparent MW (kDa)	Relative percentage (%)
>1,000	4	>1,000	11
430	ND*	430	12
259	52	259	ND
89	ND	89	18
54	44	54	59

*ND, not detected.

of oxidized p53 was in the monomer form (59%, MW = 54 kDa), and the majority of the reduced p53 was in the tetramer form (52%, MW = 259 kDa). We note that oxidized p53 also formed dimers (18%, MW = 89 kDa), intermediate size oligomers (12%, MW = 430 kDa), and higher ordered protein complexes (11%, MW > 1,000 kDa), but no tetramers. Reduced p53, aside from tetramers, also formed monomers (44%, MW = 54 kDa), but very little higher ordered protein complexes (4%, MW > 1,000 kDa). The data indicate that reduced p53 has a higher propensity to form tetramers than oxidized p53 and is consistent with a model in which oxidation prevents proper tetramerization of p53. We cannot rule out the possibility that the intermediate size oligomers (MW = 430 kDa) of oxidized p53 are actually tetramers with an unusual conformation. Tetramers of this approximate apparent MW were previously observed (9). The possibility that unusually shaped tetramers were present in the oxidized p53 sample was confirmed by glutaraldehyde cross-linking studies (data not shown). Oxidized p53 tends to form high MW complexes of >1,000 kDa and intermediate size oligomers and/or unusually shaped tetramers. Because tetrameric p53 is the most efficient at binding DNA (30), it is likely that inhibition of proper tetramer formation of the 259 kDa MW size explains why oxidized p53 fails to bind DNA efficiently.

Oxidized p53 thiol groups are more susceptible to MAL-PEG conjugation than reduced p53

The data suggest that a single surface thiol group forms a disulfide bond under relatively mild oxidizing conditions. A previous study using conformation-specific antibodies showed that oxidation promotes a conformation change in p53 (11). To confirm and extend these studies, we performed a conformation analysis experiment using the thiol probe MAL-PEG. MAL-PEG forms a thioether bond with cysteine thiol groups on the protein surface. The MAL-PEG bound form of p53 can easily be distinguished from unbound p53 after separation by SDS-PAGE because each MAL-PEG adduct increases the MW of the polypeptide by ~5,000 Da (18). However, due to its bulky structure, MAL-PEG will not react efficiently with the protein if the reactive thiol groups are partially occluded or are in close proximity to each other. Figure 5 shows that when reduced p53 was incubated with 0.67 m*M* MAL-PEG, 32% formed adducts. At 1.3 m*M* MAL-PEG, 71% of p53 formed adducts, and at 3.3 m*M* MAL-PEG, 81% of p53 formed adducts. MAL-PEG adduct formation with oxidized p53 was more efficient than adduct formation with reduced p53. At 0.67 m*M* MAL-PEG, 95% of oxidized p53 formed adducts. At 1.3 m*M* and 3.3 m*M,* 100% of p53 formed adducts. The relative lack of MAL-PEG reactivity by reduced p53 suggests that its thiol groups are sterically blocked and unavailable for reaction with the bulky adduct. Oxidized p53, on the other hand, is more likely to be in the monomer stage or exhibit a conformation that is available for reaction with MAL-PEG, thus, its greater degree of reactivity. We note that at 0.67 m*M* and 1.3 m*M* MAL-PEG, 23% and 43% of oxidized p53, respectively, formed more than four adducts. Reduced p53 failed to form more than four adducts at lower MAL-PEG concentrations. We suggest that oxidized p53, when bound to more than one MAL-PEG molecule, is susceptible to denaturation, which allows its buried cysteine thiols to be available for additional MAL-PEG adduct formation. Reduced p53, on the other hand, is less susceptible to MAL-PEG adduct formation due to the fact that its thiol groups are located on the interface of the p53 subunits.

Testable model for oxidation of p53 at Cys182

The results suggest the possibility that p53 may bind one small thiol-containing molecule that could prevent it from binding DNA and decrease tetramer formation. One common small thiol group is glutathione, a thiol-containing tripeptide that has been demonstrated to form protein disulfide adducts in cells that are oxidatively stressed (27). Although we have demonstrated that five cysteine thiol groups are exposed on the surface of the protein, Cys182 is located in an ideal location to inhibit DNA binding and alter the quaternary structure. By using x-ray crystallography data (4), a model was built depicting the arrangement of two p53 DNA binding domains binding to two pentamer consensus sequences. Figure 6A shows that these two subunits each interact with the major groove of the DNA and that the helices containing Cys182 come into close proximity to each other, in agreement with recent solution structure data (15). These short helices are composed of residues Pro177-Cys182. As shown in Fig. 6B, if glutathione were to form a disulfide bond to each of two Cys182 residues, the two subunits would dissociate laterally by as much as several angstroms. This lateral motion would disengage the p53 from the DNA. Although not depicted in the model, such a displacement would also be expected to disrupt the tetramerization domain, which is located further toward the C-terminus.

DISCUSSION

The cysteine thiol groups predicted to be exposed on the surface of native p53 and thus most likely involved in p53 functionality are Cys176, Cys182, Cys229, Cys242, and Cys277 (31). Cys176 and Cys242 join Cys238 in coordinating a zinc atom and, together, are required for maintenance of the ter-

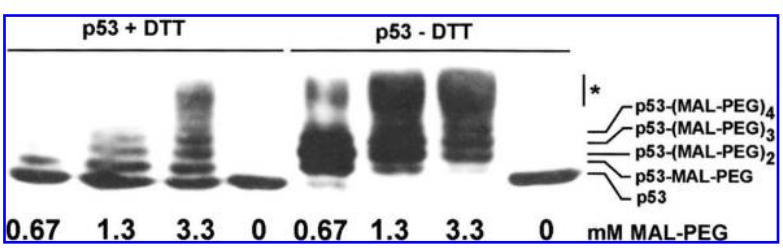

FIG. 5. Demonstration of p53 conformation changes by DTT. Reduced p53 and oxidized p53 were treated with the indicated concentrations of MAL-PEG for 30 min at 25°C. MAL-PEG binding reaction was quenched by addition of hot Laemmli protein sample buffer, and proteins were separated by SDS-PAGE. p53 was detected by western analysis with DO-1 antibody. Asterisk represents p53 bound to more than five MAL-PEG adducts.

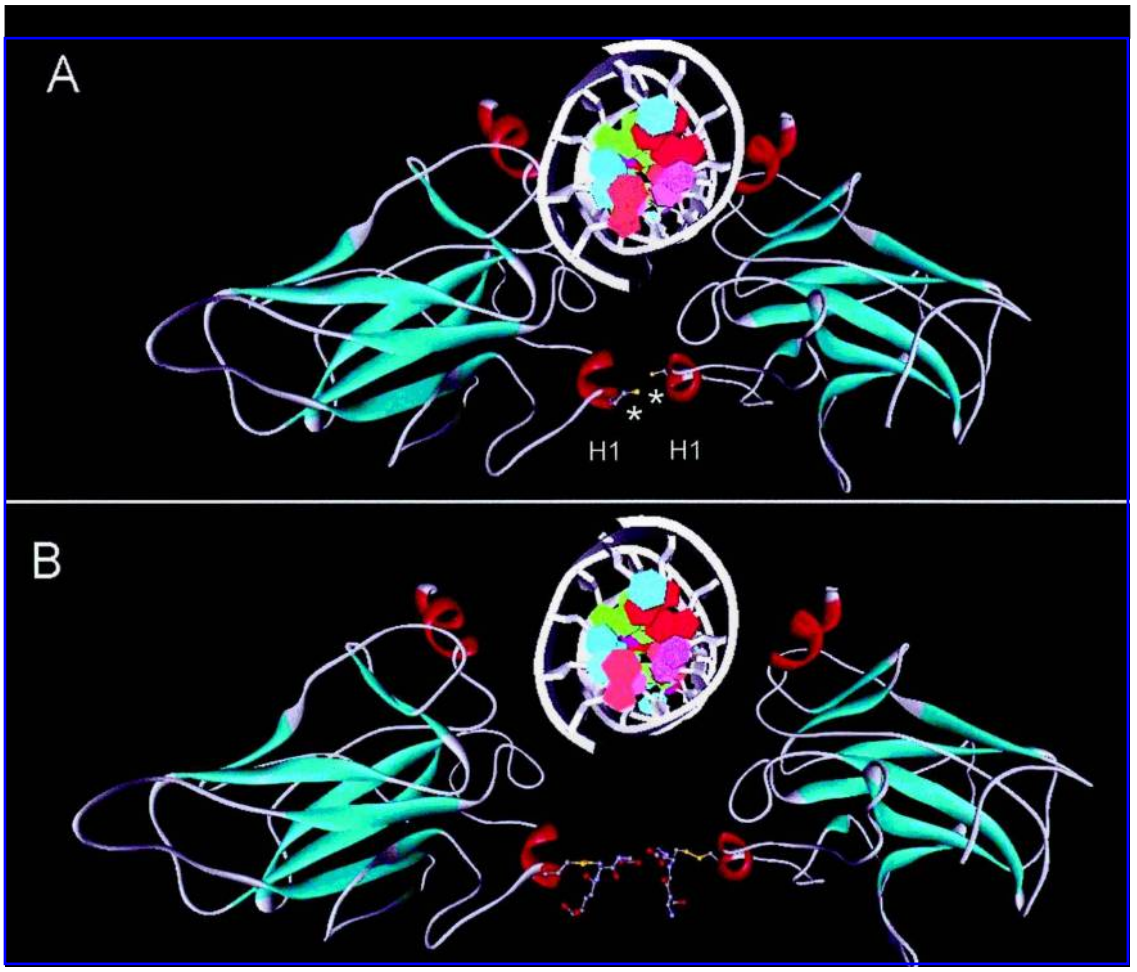

FIG. 6. Hypothetic model of how glutathione bound to Cys182 of p53 could disrupt quaternary interactions. (**A**) Two p53 DNA binding domains engaging two pentamers within the DNA consensus sequence (projecting perpendicular to the plane of the page). The dimer of the p53 DNA binding domains are partially stabilized by H1 helix/H1 helix interactions (labeled H1), and Cys182 (asterisks) on each H1 helix is directed into the opposing H1 helix. (**B**) When glutathione is bound to Cys182, the H1 helices are incapable of interacting and the two DNA binding domains disengage the DNA consensus sequence. For clarity, the p53 subunits are shown in the conceptual solid ribbon format and the DNA in the ladder format. Only the Cys182 residues and the bound glutathione molecules are depicted at atomic level resolution (lacking hydrogen atoms) in the ball and stick format.

tiary structure necessary for p53 to bind DNA in a sequence-specific fashion (4). Cys277 makes direct contact to N4 of cytosine or O4 of thymine within a p53 DNA consensus sequence. Cys182 is located within a region where two p53 DNA binding domains associate called the H1 helix (15).

The DTNB derivatization results show that five thiols are present on the surface of reduced p53 and four on oxidized p53. A single disulfide bond per p53 is observed, and there is no evidence of intersubunit disulfide bonds. This result, unexpected because one would expect two surface thiols to become oxidized to form a disulfide bridge, can be explained in one of two ways. First, one cysteine can form a disulfide bond intramolecularly with a cysteine sulfhydryl that is partially buried and thus undetectable in the DTNB study. This may be the case with Cys277 (surface) and Cys275 (buried) because they are in close proximity to each other and, although Cys275 is not completely exposed to the surface, it may be able to undergo a conformation change to accommodate a disulfide bridge with Cys277. The surface to buried disulfide bonding may also be the case with zinc binding residues Cys176 (surface), Cys238 (buried), and Cys242 (surface). Disulfide bond formation between any two of these cysteine residues would likely expel zinc and lead to a global conformation change consistent with our conformation analysis data.

The second explanation would be that there is an intermolecular disulfide bond between a surface cysteine thiol and a small, sulfhydryl-containing molecule such as glutathione. In this case, it may be difficult to tell which surface cysteine participates in the disulfide linkage. In accordance with our AFM, MAL-PEG, and gel filtration data, the reactive cysteine sulfhydryl would most likely be in a position that is important for proper tertiary or quaternary structure formation. Specifically, the small molecule must inhibit DNA binding and expose other surface cysteine thiol groups to the surface, as well as inhibit tetramer formation. In our modeling study (see Fig. 6), it was shown that if such a small molecule, in this case glutathione, were to bind Cys182, the H1 helix of each p53 DNA binding domain would be pushed away from each

other. The p53 dimer would be incapable of binding to DNA and, furthermore, may be inhibited in its ability to form a tetramer. In the absence of DNA, the subunits of reduced p53 may partially block thiol groups from exposure to large thiol-reacting molecules such as MAL-PEG. This may explain why MAL-PEG fails to react with reduced p53. With glutathione bound to Cys182, we speculate that the p53 monomers are less able to protect each other's thiol groups and are more susceptible to MAL-PEG conjugation. However, we cannot rule out the possibility that a small molecule could form a disulfide bond with other surface cysteine residues; but it is not clear whether such binding would lead to the gross conformation alterations detected in our study. It is also possible that no one particular cysteine residue is oxidized to the exclusion of others in a population of p53 molecules nor can we exclude the possibility that a subpopulation of the p53 contains more than one oxidized surface thiol and the other subpopulation is reduced. The gel filtration data show that oxidized p53 exists in a variety of oligomeric forms, including monomers, dimers, and large aggregates. Oxidized p53 appears to also form a tetramer that has a shape that is distinct from reduced p53. Each oxidized species may be formed from a particular cysteine residue oxidation.

We have ruled out significant contributions of other types of oxidation to p53 under our conditions. Specifically, we ruled out sulfenic acid, sulfinic acid, and sulfonic acid as major contributors to oxidation of p53. Interestingly, we detected a substoichiometric level of sulfinic acid in the oxidized p53 (approximately 1:10 molar ratio). Sulfinic acid is not reduced to the sulfhydryl by the addition of DTT. However, as addition of DTT to oxidized p53 increases DNA binding capacity, this indicates that sulfinic acid does not significantly contribute to inhibition of DNA binding. One type of oxidation we have not ruled out is nitrosylation.

A tetramer at p53 binds to a full consensus site consisting of four pentamers. The p53 particles observed to be bound to DNA in our AFM studies have dimensions consistent with that expected for a tetramer if one considers that one dimer binds a half-site on an oligonucleotide and a second dimer binds to another half-site on a different oligonucleotide. Our AFM data are consistent with a recent NMR/modeling study in which this sandwich-like model was suggested (15). According to this model, the p53 tetramer straddles between two half-sites and engages each at an approximate 90° angle. An electron microscopy analysis of p53 bound to DNA showed that the distance between the two DNAs is 10 nm (25). Considering that the diameter of B-DNA is 2.4 nm (1), and that p53 wraps itself approximately half way around the consensus site, one would expect that the p53 tetramer cross-section distance to be ~8 nm. This measurement is remarkably consistent with our measurement of 8.61 nm for the tetramer. In our experimental setup, it is likely that p53 tetramer binds a single half-site through one dimer while the second dimer is not bound to DNA. The height of p53 is ~4.12 nm with very little variation. This distance is slightly larger than one turn of B-DNA (3.4 nm), which would code for a half-site. The data indicate that the p53 tetramer is a flat disc that engages the DNA perpendicularly. As predicted, the number of oxidized p53 particles bound to DNA detected by AFM was lower by ninefold. Whether this is due to a decrease in the rate of binding or due to a higher dissociation constant is not clear. The oxidized p53 particles that bind DNA possess a longer diameter (15.32 nm) and decreased height (3.14 nm) and much greater variation compared with reduced p53 particles. This may suggest that, upon oxidation, p53 assumes a more open conformation that expands the disc shape, but does not greatly affect the height of the tetramer. The fact that oxidized p53 appears to have a larger Stokes radius (apparent MW 430 kDa versus 259 kDa) lends credence to this idea. Glutaraldehyde cross-linking experiments by us (data not shown) and others (9) suggest that at least some oxidized p53 retains a tetrameric state.

Perspective

Oxidation appears to regulate p53's ability to bind a consensus sequence. A recent report has shown that selenomethionine and Redox factor-1 can maintain p53 in a reduced state within cultured cells (24). This study suggests that Cys275 and/or Cys277 are susceptible to reversible oxidation in the absence of selenomethionine and Redox factor-1; but other cysteine residue thiols have not been excluded. Another study suggests that Cys277 is susceptible to oxidation in UV-damaged cells and that oxidation prevents the p53 from binding *GADD45* promoter (2). Previous work has demonstrated that free radicals produced by the Fenton reaction in the presence of copper can oxidize p53 both in cells and *in vitro* (10). Future studies will be required to uncover the specific sites of cysteine residue oxidation on p53, the oxidizing ligand, and the mechanism of oxidation.

ACKNOWLEDGMENTS

This work was supported by grants from the Minorities in Biomedical Research Sciences Program (NIGMS08101) and the Bridges-to-the-Future Program (NIGMS49001) of the National Institutes of Health. We thank Dr. Gerard Zambetti (St. Jude Children's Research Hospital, Memphis, TN, U.S.A.) for the generous gift of the p53 baculovirus and Dr. Susan Kane for critical reading of the manuscript.

ABBREVIATIONS

AFM, atomic force microscopy; APTES, aminopropyltriethoxysilane; DTNB, 5,5'-dithiobis(2-nitrobenzoic acid); DTT, dithiothreitol; Gu-SCN, guanidine isothiocyanate; MAC-mode, magnetic altering current mode; MAL-PEG, methoxymaleimide polyethylene glycol (2 kDa); MW, molecular weight; NBD chloride, 4-chloro-7-nitrobenz-2-oxa-1,3-diazole; NTB, 2-nitro-5-thiobenzoic acid; NTSB, 2-nitro-5-thiolsulfobenzoate; SDS-PAGE, sodium dodecyl sulfate–polyacrylamide gel electrophoresis.

REFERENCES

1. Berg JM, Tymoczko JL, and Stryer L. *Biochemistry.* New York: W.H. Freeman and Company, 2001, p. 750.
2. Buzek J, Latonen L, Kurki S, Peltonen K, and Laiho M. Redox state of tumor suppressor p53 regulates its sequence-

specific DNA binding in DNA-damaged cells by cysteine 277. *Nucleic Acids Res* 30: 2340–2348, 2002.
3. Chene P. Mutations at position 277 modify the DNA-binding specificity of human p53 *in vitro*. *Biochem Biophys Res Commun* 263: 1–5, 1999.
4. Cho Y, Gorina S, Jeffrey PD, and Pavletich NP. Crystal structure of a p53 tumor suppressor–DNA complex: understanding tumorigenic mutations. *Science* 265: 346–355, 1994.
5. Claiborne A, Mallet TC, Yeh JI, Luba J, and Parsonage D. Structural, redox, and mechanistic parameters for cysteine-sulfenic acid function in catalysis and regulation. *Adv Protein Chem* 58: 215–276, 2001.
6. Delphin C, Cahen P, Lawrence JJ, and Baudier J. Characterization of baculovirus recombinant wild-type p53. Dimerization of p53 is required for high-affinity DNA binding and cysteine oxidation inhibits p53 DNA binding. *Eur J Biochem* 223: 683–692, 1994.
7. Ellis HR and Poole LB. Novel application of 7-chloro-4-nitrobenzo-2-oxa-1,3-diazole to identify cysteine sulfenic acid in the AhpC component of alkyl hydroperoxide reductase. *Biochemistry* 36: 15013–15018, 1997.
8. Ellman GL. Tissue sulfhydryl groups. *Arch Biochem Biophys* 82: 70–77, 1959.
9. Friedman PN, Chen X, Bargonetti J, and Prives C. The p53 protein is an unusually shaped tetramer that binds directly to DNA. *Proc Natl Acad Sci U S A* 90: 3319–3323, 1993.
10. Furuta S, Ortiz F, Sun XZ, Wu HH, Mason A, and Momand J. Copper uptake is required for pyrrolidine dithiocarbamate-mediated oxidation and protein level increase of p53 in cells. *Biochem J* 365: 639–648, 2002.
11. Hainaut P and Milner J. Redox modulation of p53 conformation and sequence-specific DNA binding in vitro. *Cancer Res* 53: 4469–4473, 1993.
12. Hamann M, Zhang T, Hendrich S, and Thomas JA. Quantitation of protein sulfinic and sulfonic acid, irreversibly oxidized protein cysteine sites in cellular proteins. *Methods Enzymol* 348: 146–156, 2002.
13. Jayaraman L, Murthy KG, Zhu C, Curran T, Xanthoudakis S, and Prives C. Identification of redox/repair protein Ref-1 as a potent activator of p53. *Genes Dev* 11: 558–570, 1997.
14. Kim SO, Merchant K, Nudelman R, Beyer WF Jr, Keng T, DeAngelo J, Hausladen A, and Stamler JS. OxyR: a molecular code for redox-related signaling. *Cell* 109: 383–396, 2002.
15. Klein C, Planker E, Diercks T, Kessler H, Kunkele KP, Lang K, Hansen S, and Schwaiger M. NMR spectroscopy reveals the solution dimerization interface of p53 core domains bound to their consensus DNA. *J Biol Chem* 276: 49020–49027, 2001.
16. Levine AJ. p53, the cellular gatekeeper for growth and division. *Cell* 88: 323–331, 1997.
17. Levine AJ, Momand J, and Finlay CA. The p53 tumour suppressor gene. *Nature* 351: 453–456, 1991.
18. Makmura L, Hamman M, Areopagita A, Furuta S, Muñoz A, and Momand J. Development of a sensitive assay to detect reversibly oxidized cysteine sulfhydryl groups. *Antioxid Redox Signal* 3: 1105–1118, 2001.
19. Marquett CA, Lawrence I, Polychronakos C, and Lawrence MF. Impedance based DNA chip for direct Tm measurement. *Talanta* 56: 763–768, 2002.
20. McLure KG and Lee PW. How p53 binds DNA as a tetramer. *EMBO J* 17: 3342–3350, 1998.
21. Oh SJ, Cho SJ, Kim CO, and Park JW. Characteristics of DNA microarrays fabricated on various aminosilane layers. *Langmuir* 18: 1764–1769, 2002.
22. Olivier M, Eeles R, Hollstein M, Khan MA, Harris CC, and Hainaut P. The IARC TP53 database: new online mutation analysis and recommendations to users. *Hum Mutat* 19: 607–614, 2002.
23. Rainwater R, Parks D, Anderson ME, Tegtmeyer P, and Mann K. Role of cysteine residues in regulation of p53 function. *Mol Cell Biol* 15: 3892–3903, 1995.
24. Seo YR, Kelley MR, and Smith ML. Selenomethionine regulation of p53 by a ref1-dependent redox mechanism. *Proc Natl Acad Sci U S A* 99: 14548–14553, 2002.
25. Stenger JE, Tegtmeyer P, Mayr GA, Reed M, Wang Y, Wang P, Hough PV, and Mastrangelo IA. p53 oligomerization and DNA looping are linked with transcriptional activation. *EMBO J* 13: 6011–6020, 1994.
26. Thannhauser TW, Konishi Y, and Scheraga HA. Sensitive quantitative analysis of disulfide bonds in polypeptides and proteins. *Anal Biochem* 138: 181–188, 1984.
27. Thomas JA, Poland B, and Honzatko R. Protein sulfhydryls and their role in the antioxidant function of protein *S*-thiolation. *Arch Biochem Biophys* 319: 1–9, 1995.
28. Tyner SD, Venkatachalam S, Choi J, Jones S, Ghebranious N, Igelmann H, Lu X, Soron G, Cooper B, Brayton C, Hee Park S, Thompson T, Karsenty G, Bradley A, and Donehower LA. p53 mutant mice that display early ageing-associated phenotypes. *Nature* 415: 45–53, 2002.
29. Ueno M, Masutani H, Arai RJ, Yamauchi A, Hirota K, Sakai T, Inamoto T, Yamaoka Y, Yodoi J, and Nikaido T. Thioredoxin-dependent redox regulation of p53-mediated p21 activation. *J Biol Chem* 274: 35809–35815, 1999.
30. Wang Y, Schwedes JF, Parks D, Mann K, and Tegtmeyer P. Interaction of p53 with its consensus DNA-binding site. *Mol Cell Biol* 15: 2157–2165, 1995.
31. Wu HH, Sherman M, Yuan YC, and Momand J. Direct redox modulation of p53 protein: potential sources of redox control and potential outcomes. *Gene Ther Mol Biology* 4: 119–132, 1999.

Address reprint requests to:
Dr. Jamil Momand
Department of Chemistry and Biochemistry
California State University
Los Angeles, CA 90032

E-mail: jmomand@calstatela.edu

Received for publication April 21, 2003; accepted July 8, 2003.

This article has been cited by:

1. Dr. Daniela De Zio , Prof. Francesco Cecconi , Dr. Valentina Cianfanelli . New insights into the link between DNA Damage and Apoptosis. *Antioxidants & Redox Signaling* **0**:ja. . [Abstract] [Full Text PDF] [Full Text PDF with Links]
2. Jie Zhuang, Wenzhe Ma, Cory U. Lago, Paul M. Hwang. 2012. Metabolic regulation of oxygen and redox homeostasis by p53: Lessons from evolutionary biology?. *Free Radical Biology and Medicine* **53**:6, 1279-1285. [CrossRef]
3. E.A. Ostrakhovitch, O.A. Semenikhin. 2012. The role of redox environment in neurogenic development. *Archives of Biochemistry and Biophysics* . [CrossRef]
4. Aaron K. Holley, Sanjit Kumar Dhar, Daret K. St. Clair. 2012. Curbing cancer's sweet tooth: Is there a role for MnSOD in regulation of the Warburg effect?. *Mitochondrion* . [CrossRef]
5. Beyza Vurusaner, Giuseppe Poli, Huveyda Basaga. 2012. Tumor suppressor genes and ROS: complex networks of interactions. *Free Radical Biology and Medicine* **52**:1, 7-18. [CrossRef]
6. Cory U. Lago , Ho Joong Sung , Wenzhe Ma , Ping-yuan Wang , Paul M. Hwang . 2011. p53, Aerobic Metabolism, and Cancer. *Antioxidants & Redox Signaling* **15**:6, 1739-1748. [Abstract] [Full Text HTML] [Full Text PDF] [Full Text PDF with Links]
7. Merridee A. Wouters, Siiri Iismaa, Samuel W. Fan, Naomi L. Haworth. 2011. Thiol-based redox signalling: Rust never sleeps. *The International Journal of Biochemistry & Cell Biology* **43**:8, 1079-1085. [CrossRef]
8. Jenna Scotcher, David J. Clarke, Stefan K. Weidt, C. Logan Mackay, Ted R. Hupp, Peter J. Sadler, Pat R. R. Langridge-Smith. 2011. Identification of Two Reactive Cysteine Residues in the Tumor Suppressor Protein p53 Using Top-Down FTICR Mass Spectrometry. *Journal of The American Society for Mass Spectrometry* **22**:5, 888-897. [CrossRef]
9. Do-Hee Kim, Joydeb Kumar Kundu, Young-Joon Surh. 2011. Redox modulation of p53: Mechanisms and functional significance. *Molecular Carcinogenesis* **50**:4, 222-234. [CrossRef]
10. Ayelet Erez, Oleg A. Shchelochkov, Sharon E. Plon, Fernando Scaglia, Brendan Lee. 2011. Insights into the Pathogenesis and Treatment of Cancer from Inborn Errors of Metabolism. *The American Journal of Human Genetics* **88**:4, 402-421. [CrossRef]
11. A. O. Zheltukhin, P. M. Chumakov. 2010. Constitutive and induced functions of the p53 gene. *Biochemistry (Moscow)* **75**:13, 1692-1721. [CrossRef]
12. Joseph Shlomai . 2010. Redox Control of Protein–DNA Interactions: From Molecular Mechanisms to Significance in Signal Transduction, Gene Expression, and DNA Replication. *Antioxidants & Redox Signaling* **13**:9, 1429-1476. [Abstract] [Full Text HTML] [Full Text PDF] [Full Text PDF with Links]
13. Young-Mi Go , Dean P. Jones . 2010. Redox Control Systems in the Nucleus: Mechanisms and Functions. *Antioxidants & Redox Signaling* **13**:4, 489-509. [Abstract] [Full Text HTML] [Full Text PDF] [Full Text PDF with Links]
14. A Salmeen, B O Park, T Meyer. 2010. The NADPH oxidases NOX4 and DUOX2 regulate cell cycle entry via a p53-dependent pathway. *Oncogene* **29**:31, 4473-4484. [CrossRef]
15. Sergio Rosales-Corral , Russel J. Reiter , Dun-Xian Tan , Genaro G. Ortiz , Gabriela Lopez-Armas . 2010. Functional Aspects of Redox Control During Neuroinflammation. *Antioxidants & Redox Signaling* **13**:2, 193-247. [Abstract] [Full Text HTML] [Full Text PDF] [Full Text PDF with Links]
16. Wayne Chris Hawkes, Zeynep Alkan. 2010. Regulation of Redox Signaling by Selenoproteins. *Biological Trace Element Research* **134**:3, 235-251. [CrossRef]
17. Meghan L. Verschoor, Leigh A. Wilson, Gurmit Singh. 2010. Mechanisms associated with mitochondrial-generated reactive oxygen species in cancerThis article is one of a selection of papers published in a Special Issue on Oxidative Stress in Health and Disease. *Canadian Journal of Physiology and Pharmacology* **88**:3, 204-219. [CrossRef]

18. Ning Xia, Lin Liu, Xinyao Yi, Jianxiu Wang. 2009. Studies of interaction of tumor suppressor p53 with apo-MT using surface plasmon resonance. *Analytical and Bioanalytical Chemistry* **395**:8, 2569-2575. [CrossRef]
19. Samuel W. Fan, Richard A. George, Naomi L. Haworth, Lina L. Feng, Jason Y. Liu, Merridee A. Wouters. 2009. Conformational changes in redox pairs of protein structures. *Protein Science* **18**:8, 1745-1765. [CrossRef]
20. David W. Essex . 2009. Redox Control of Platelet Function. *Antioxidants & Redox Signaling* **11**:5, 1191-1225. [Abstract] [Full Text PDF] [Full Text PDF with Links]
21. Jeremy M.R. Lambert, Petr Gorzov, Dimitry B. Veprintsev, Maja Söderqvist, Dan Segerbäck, Jan Bergman, Alan R. Fersht, Pierre Hainaut, Klas G. Wiman, Vladimir J.N. Bykov. 2009. PRIMA-1 Reactivates Mutant p53 by Covalent Binding to the Core Domain. *Cancer Cell* **15**:5, 376-388. [CrossRef]
22. Fabio Di Domenico, Giovanna Cenini, Rukhsana Sultana, Marzia Perluigi, Daniela Uberti, Maurizio Memo, D. Allan Butterfield. 2009. Glutathionylation of the Pro-apoptotic Protein p53 in Alzheimer's Disease Brain: Implications for AD Pathogenesis. *Neurochemical Research* **34**:4, 727-733. [CrossRef]
23. Aaron K Holley, Daret K St Clair. 2009. Watching the watcher: regulation of p53 by mitochondria. *Future Oncology* **5**:1, 117-130. [CrossRef]
24. Yongping Pan, Ruth Nussinov. 2009. Preferred drifting along the DNA major groove and cooperative anchoring of the p53 core domain: mechanisms and scenarios. *Journal of Molecular Recognition* n/a-n/a. [CrossRef]
25. Yvonne M.W. Janssen-Heininger, Brooke T. Mossman, Nicholas H. Heintz, Henry J. Forman, Balaraman Kalyanaraman, Toren Finkel, Jonathan S. Stamler, Sue Goo Rhee, Albert van der Vliet. 2008. Redox-based regulation of signal transduction: Principles, pitfalls, and promises. *Free Radical Biology and Medicine* **45**:1, 1-17. [CrossRef]
26. N ZACHE, J LAMBERT, N ROKAEUS, J SHEN, P HAINAUT, J BERGMAN, K WIMAN, V BYKOV. 2008. Mutant p53 targeting by the low molecular weight compound STIMA-1. *Molecular Oncology* **2**:1, 70-80. [CrossRef]
27. Bin Liu, Yumin Chen, Daret K. St. Clair. 2008. ROS and p53: A versatile partnership. *Free Radical Biology and Medicine* **44**:8, 1529-1535. [CrossRef]
28. G Filomeni, G Rotilio, M R Ciriolo. 2005. Disulfide relays and phosphorylative cascades: partners in redox-mediated signaling pathways. *Cell Death and Differentiation* **12**:12, 1555-1563. [CrossRef]
29. Yunfeng Wang, Xu Zhu, Zhongbo Hu, Jianxiu Wang, Feimeng Zhou. 2005. Voltammetric Determination of Surface-Confined Biomolecules withN-(2-Ethyl-ferrocene)maleimide. *Electroanalysis* **17**:23, 2163-2169. [CrossRef]
30. Suryakant K. Niture, Chinavenmeni S. Velu, Nathan I. Bailey, Kalkunte S. Srivenugopal. 2005. S-Thiolation mimicry: Quantitative and kinetic analysis of redox status of protein cysteines by glutathione-affinity chromatography. *Archives of Biochemistry and Biophysics* **444**:2, 174-184. [CrossRef]
31. Rodney E. Shackelford , Alexandra N. Heinloth , Steven C. Heard , Richard S. Paules . 2005. Cellular and Molecular Targets of Protein S-Glutathiolation. *Antioxidants & Redox Signaling* **7**:7-8, 940-950. [Abstract] [Full Text PDF] [Full Text PDF with Links]
32. Janet V. Cross, Dennis J. Templeton. 2004. Thiol oxidation of cell signaling proteins: Controlling an apoptotic equilibrium. *Journal of Cellular Biochemistry* **93**:1, 104-111. [CrossRef]
33. Helene Pelicano, Dennis Carney, Peng Huang. 2004. ROS stress in cancer cells and therapeutic implications. *Drug Resistance Updates* **7**:2, 97-110. [CrossRef]